SUPPLEMENTARY INFORMATION

Overlapping Chromatin Remodeling Systems Collaborate Genome-wide at Dynamic Chromatin Transitions

Stephanie A. Morris et al.
Laboratory of Receptor Biology and Gene Expression, National Cancer Institute, NIH

This file includes:

Supplementary Figures 1 to 10

Supplementary Tables 1 and 2

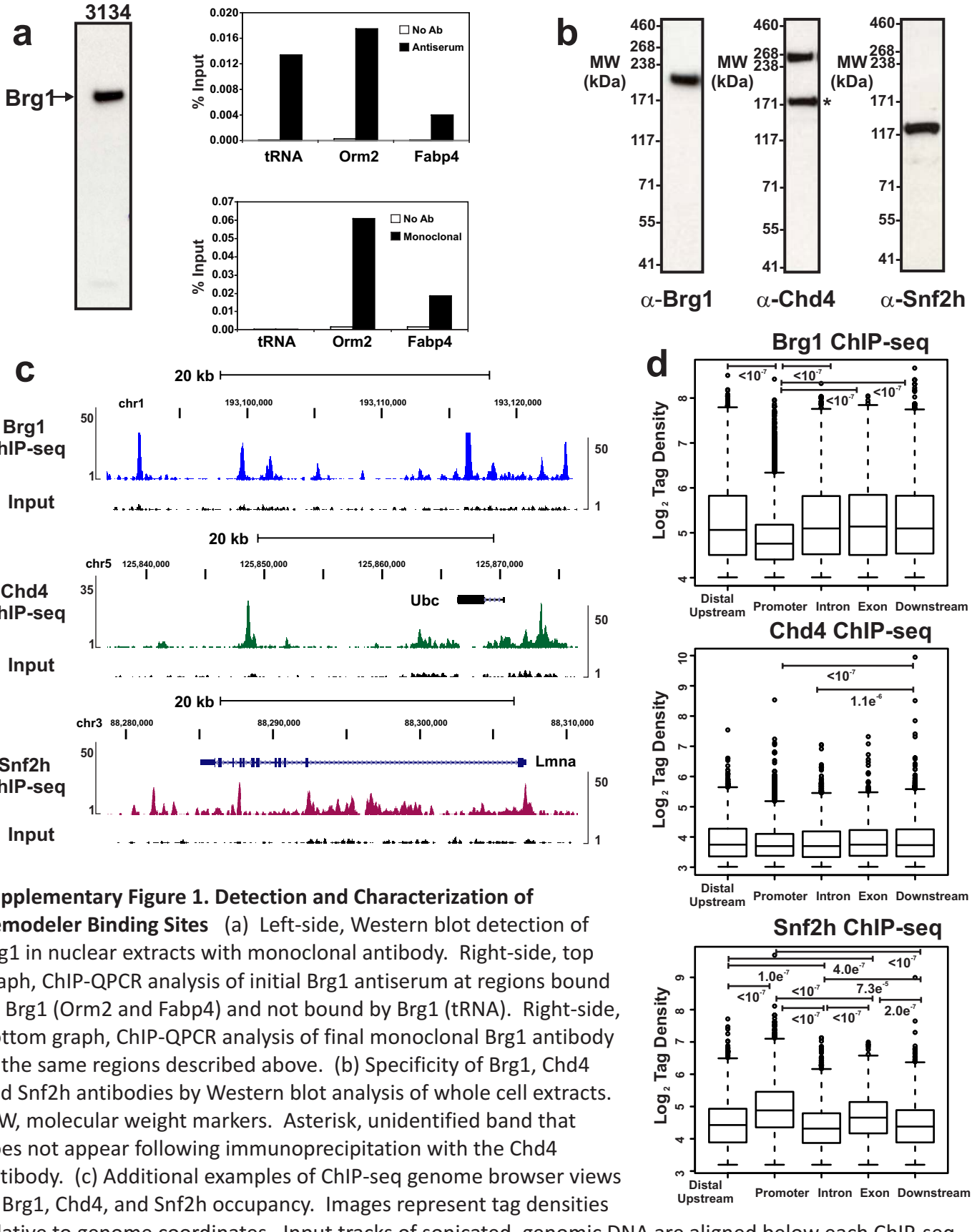

Supplementary Figure 1. Detection and Characterization of Remodeler Binding Sites (a) Left-side, Western blot detection of Brg1 in nuclear extracts with monoclonal antibody. Right-side, top graph, ChIP-QPCR analysis of initial Brg1 antiserum at regions bound by Brg1 (Orm2 and Fabp4) and not bound by Brg1 (tRNA). Right-side, bottom graph, ChIP-QPCR analysis of final monoclonal Brg1 antibody at the same regions described above. (b) Specificity of Brg1, Chd4 and Snf2h antibodies by Western blot analysis of whole cell extracts. MW, molecular weight markers. Asterisk, unidentified band that does not appear following immunoprecipitation with the Chd4 antibody. (c) Additional examples of ChIP-seq genome browser views of Brg1, Chd4, and Snf2h occupancy. Images represent tag densities relative to genome coordinates. Input tracks of sonicated, genomic DNA are aligned below each ChIP-seq track. (d) Box plots of tag density enrichment (log2 scale) of remodeler binding sites located at the indicated genomic regions. Sites are classified as promoter (< 2.5 kb upstream or downstream from the nearest TSS), exon (> 2.5 kb downstream from the nearest TSS , overlapping an exon), intron (> 2.5 kb downstream from the nearest TSS , in an intron not overlapping an exon), distal upstream (> 2.5 kb upstream from the nearest TSS), or downstream (> 2.5 kb downstream from the nearest TSS).

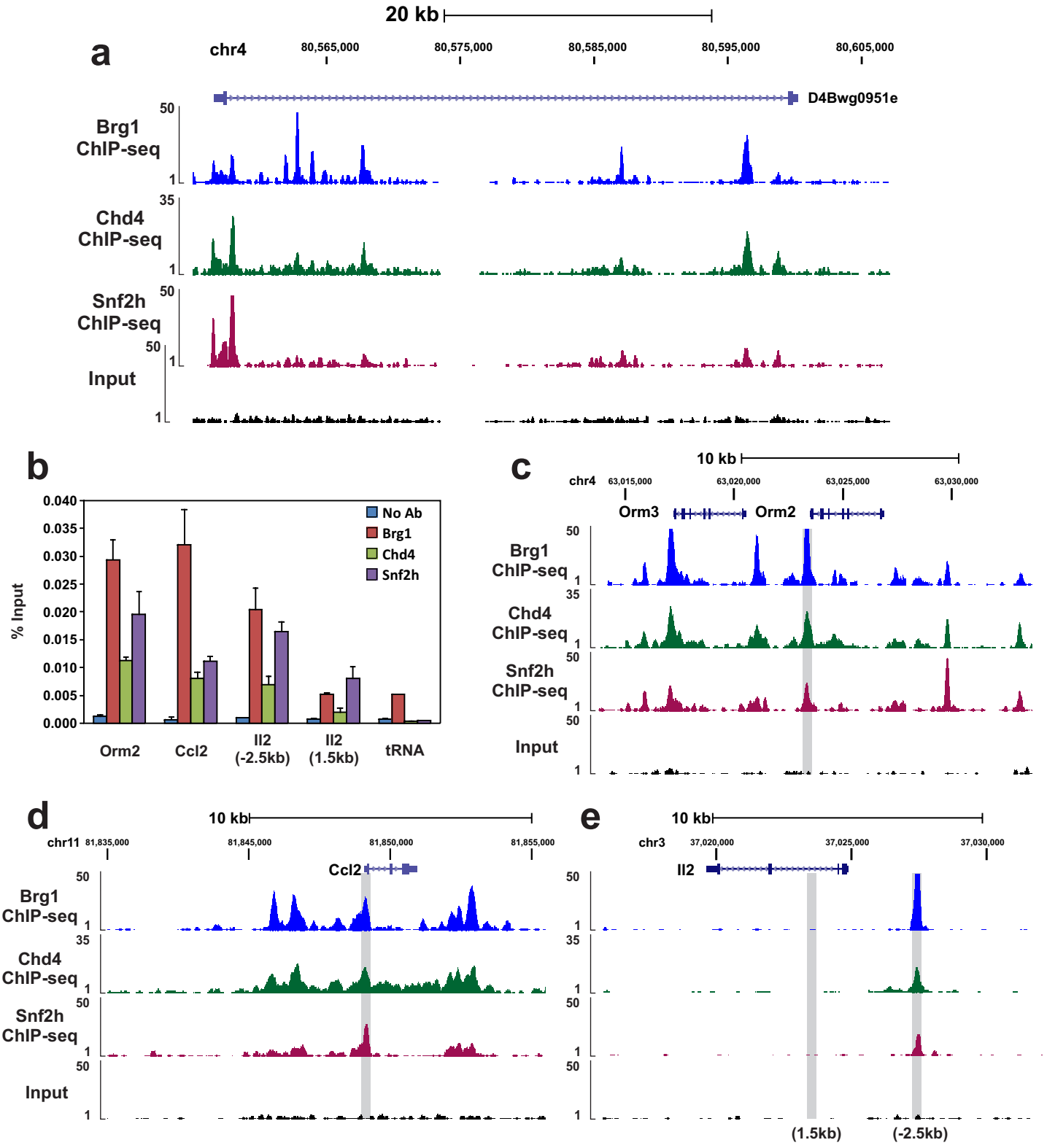

Supplementary Figure 2. Co-occupancy of Remodeler Proteins

(a) Additional example of ChIP-seq genome browser view of Brg1, Chd4, and Snf2h occupancy at the same genomic coordinates on chromosome 4. Tag density is indicated on the y-axis. (b) ChIP-QPCR analysis of Brg1, Chd4, and Snf2h at the indicated genomic regions. Bars represent the average of two replicates normalized to input DNA. No Ab, no antibody control; tRNA, negative control. Error bars represent the SEM of two independent replicates. (c-e) Genome browser view of regions analyzed in panel [(b)]. Sites amplified are highlighted in grey. Input track is included in the alignment.

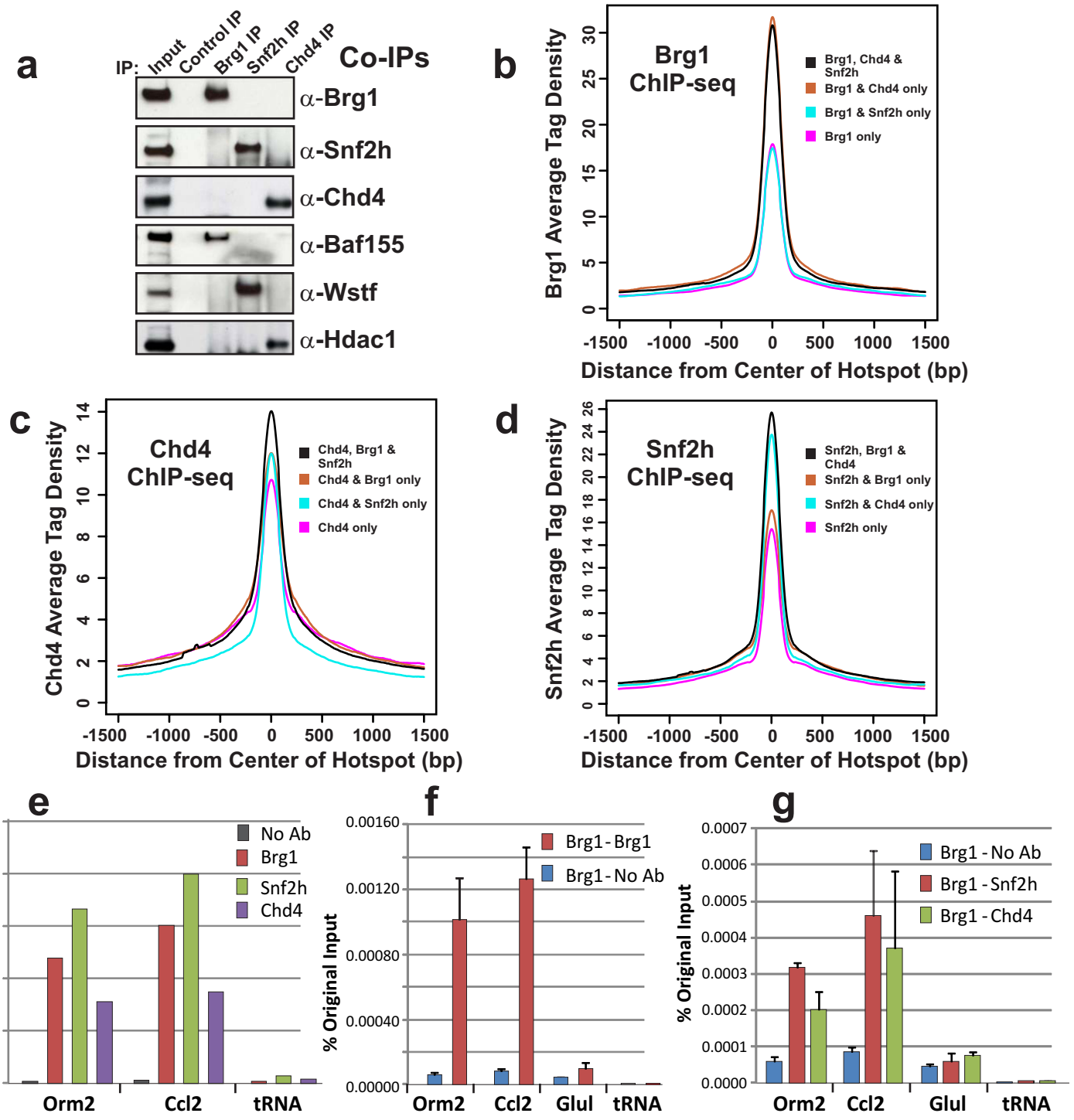

Supplementary Figure 3. Interaction of Remodeler Proteins

(a) To detect potential interactions of soluble complexes, Western blot analysis of co-immunoprecipitation (Co-IP) experiments was performed using nuclear extracts and Brg1, Snf2h, and Chd4 specific antibodies. As a control, known protein interactions were analyzed by Western (Baf155 (Brg1-associated), Wstf (Snf2h-associated), and Hdac1 (Chd4-associated). Input, 15 µg of IP nuclear extract; IP, immunoprecipitation; and control IP, lysate from 'no antibody' control sample. (b) Aggregate plot of the average tag density of Brg1 binding sites (hotspot) at regions occupied by: Brg1, Chd4, and Snf2h (black), Brg1 and Chd4 only (brown), Brg1 and Snf2h only (light blue), or Brg1 only (pink). (c) Same as in [(b)], except for Chd4 binding sites. (d) Same as in [(b and c)] for Snf2h binding sites. (e) Potential remodeler interactions at the template were examined by sequential ChIP (re-ChIP) analysis. Primary ChIP with anti-Brg1, anti-Snf2h, and anti-Chd4 was performed at the Orm2 and Ccl2 sites described in Supplementary Fig. 2b. (f) Positive control; secondary re-ChIP was performed with the anti-Brg1 IP from panel (e). (g) Secondary re-ChIP was performed with anti-Snf2h and anti-Chd4 on the anti-Brg1 IP from panel (e). Glul is a negative control site where none of the remodeler proteins were detected.

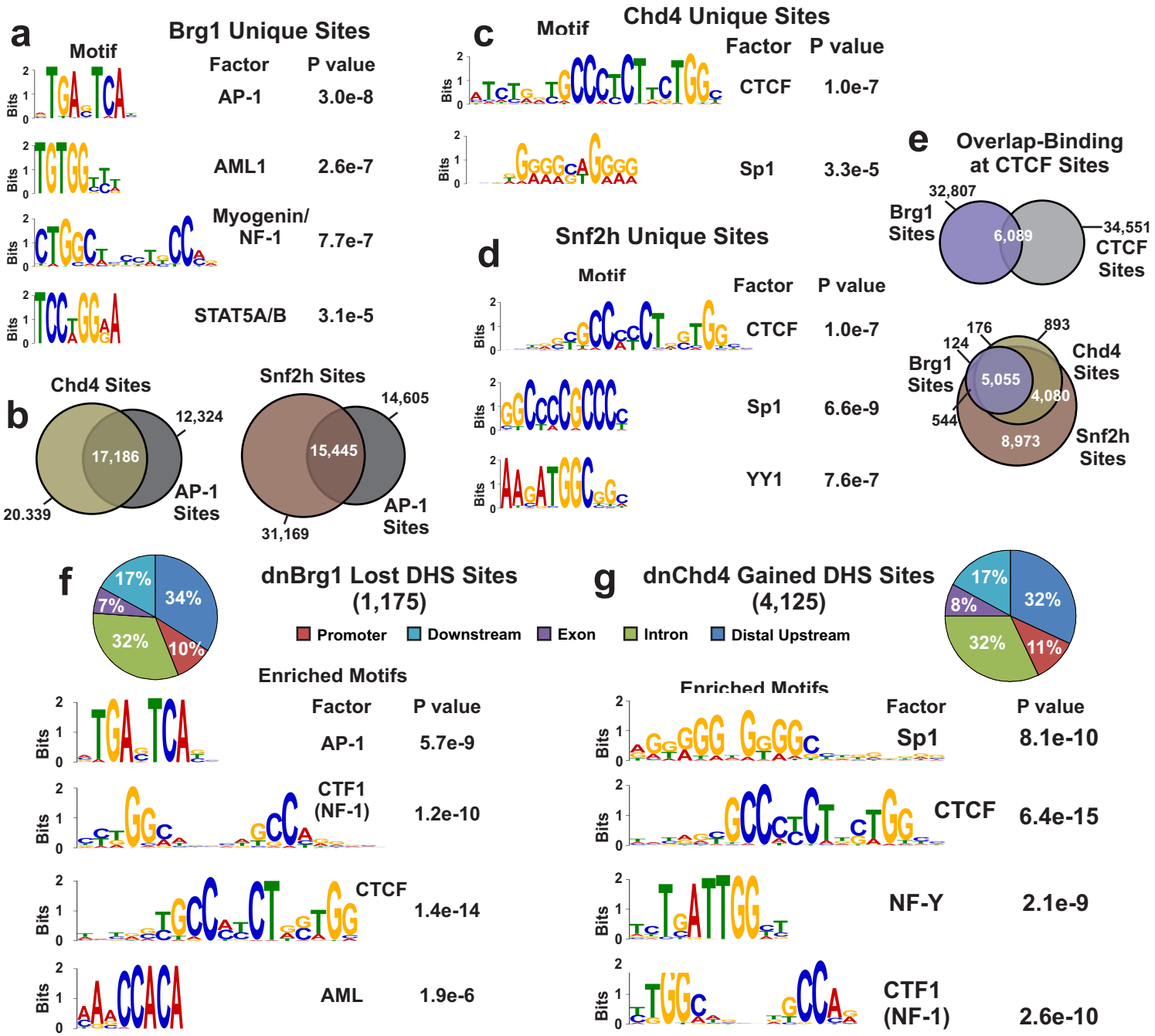

Supplementary Figure 4. De Novo Motif Analysis of Unique Remodeler Binding Sites (a) Shown are the most significantly enriched motifs associated with Brg1 unique sites (not bound by Chd4 or Snf2h) identified by MEME analysis (P < .0001) using the top 2,000 sites . The AP-1 motif was found to be the most highly enriched (MEME E value = 1.4e-1841). (b) Venn diagrams representing the overlap of binding sites for Chd4 or Snf2h with AP-1 sites. (c-d) Similar de novo motif analysis as above was performed on Chd4 and Snf2h unique sites. The CTCF motif was found to be the most highly enriched motif for Chd4 unique sites (MEME E value = 3.6e-815) and Snf2h unique sites (MEME E value = 1.1e-1026). (e) Venn diagrams of sites shared between remodelers and CTCF. Top, Venn diagram of the overlap between Brg1 and CTCF sites. Bottom, three-way Venn diagram representing the overlap between remodeler sites that specifically co-localize with CTCF sites. (f) Lost and gained DHS sites; Left-side, distribution at annotated genomic regions of DHS sites lost following the expression of dnBrg1. Bottom; Shown are the most significantly enriched motifs identified by MEME analysis (P < .0001) using the top 1,000 DHS sites (based on tag density) lost following dnBrg1 expression. The motif identified as AP-1 was found to be the most highly enriched motif (MEME E value = 1.8e-184). (g) Lost and gained DHS sites; Right-side, distribution at annotated genic regions of DHS sites gained following the expression of dnChd4. Bottom, the most significantly enriched motifs identified using the top 1,000 DHS sites (based on tag density) gained following dnChd4 expression. The motif identified as Sp1 was found to be the most highly enriched motif (MEME E value = 6.5e-167).

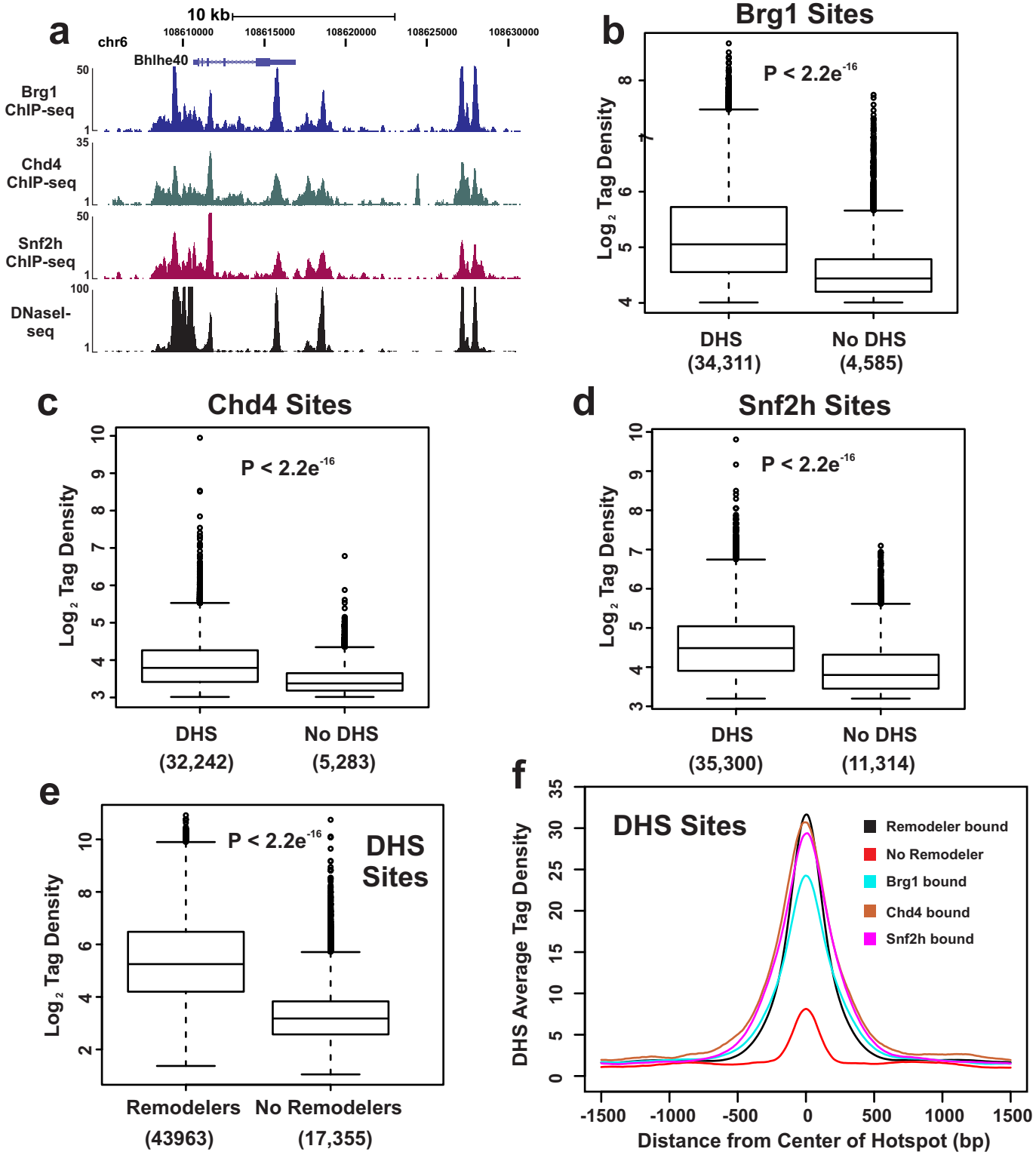

Supplementary Figure 5. Enrichment Levels of Overlapping Remodeler and DHS Sites

(a) Additional example of genome browser view displaying Brg1, Chd4, and Snf2h ChIP-seq occupancy and DNase I hypersensitivity patterns at a region on chromosome 6. (b-d) Box plots of tag density enrichment (log2 scale) of the indicated remodeler binding sites overlapping DNase I hypersensitive sites (DHS) and remodeler binding sites not associated with DHS sites. (e) Box plot of tag density enrichment (log2 scale) of DHS sites overlapping remodeler binding sites (Remodeler) and DHS sites not associated with remodeler binding. The number of each site type is indicated below the corresponding box plot. (f) Aggregate plot of the average tag density of DHS sites (hotspot) at regions occupied by: all remodelers (any/all combinations of remodeler binding, black), no remodelers (red), Brg1 only (light blue), Chd4 only (brown), or Snf2h only (pink).

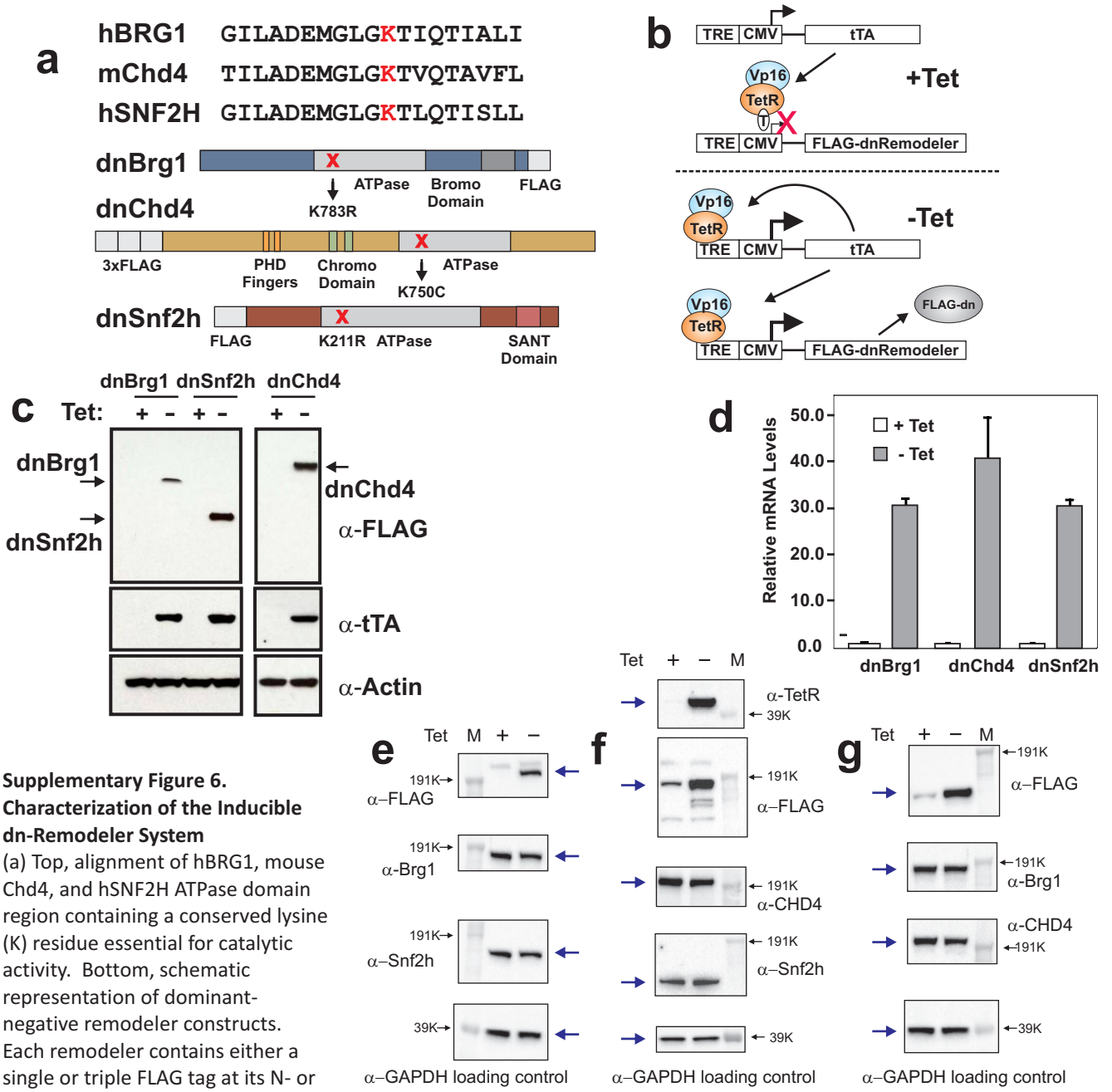

Supplementary Figure 6. Characterization of the Inducible dn-Remodeler System

(a) Top, alignment of hBRG1, mouse Chd4, and hSNF2H ATPase domain region containing a conserved lysine (K) residue essential for catalytic activity. Bottom, schematic representation of dominant-negative remodeler constructs. Each remodeler contains either a single or triple FLAG tag at its N- or C-terminus for the monitoring of expression. Highlighted is the mutation of the conserved lysine within the ATPase domain to either arginine (R) or cysteine (C). (b) Schematic of tetracycline-regulated expression system. Each dominant-negative remodeler construct was stably transfected into cells containing the tetracycline transactivator (tTA) system. The tTA construct is positioned downstream of a tetracycline (Tet) response element (TRE) bound to a minimal CMV promoter and is itself regulated by the tTA protein (Vp16-TetR) providing autoinducible control. (c) Western blot analysis of dominant-negative (dn) protein expression derived from whole cell extracts of cultured cells in the presence or absence of tetracycline (Tet). Each remodeler was FLAG-tagged at either the N- or C-terminus and detected using a FLAG-specific antibody. As a positive control, the expression of tetracycline transactivator (tTA) was analyzed (only expressed in the absence of Tet). Actin was analyzed to determine equal loading. (d) mRNA expression of dominant-negative remodelers in the presence (+Tet, white bars) or absence of tetracycline (-Tet, black bars). Expression is shown relative to the +Tet condition (no expression) with normalization to Actin expression. Error bars represent the SEM of three independent replicates. (e-g) Effect of dn-remodeler expression on levels of alternate remodeling proteins. Western blot analysis of selected remodeler expression levels with activation of alternate dn factors. Nuclear extracts from cells either expressing (- tet), or not expressing (+tet, 48 hr.), FLAG-tagged versions of dnBrg1, dnSnf2h, and dnChd4 were tested for effects on the other remodeling proteins. Input, 15 µg of IP nuclear extract; western blots were developed with antibodies specific to FLAG, Brg1, Chd4, Snf2h, the tet regulator, or GAPDH as loading control. Black arrows indicate position of size markers; blue arrows indicated position of factor tested. (e) Cells expressing dnCHD4; Brg1 and Snf2h levels are unaffected. (f) Cells expressing dnBrg1; Chd4 and Snf2h levels are unaffected. Strong induction of the tet regulator is also shown at the top of the panel. (g) Cells expressing dn Snf2h; Brg1 and Chd4 levels are unaffected.

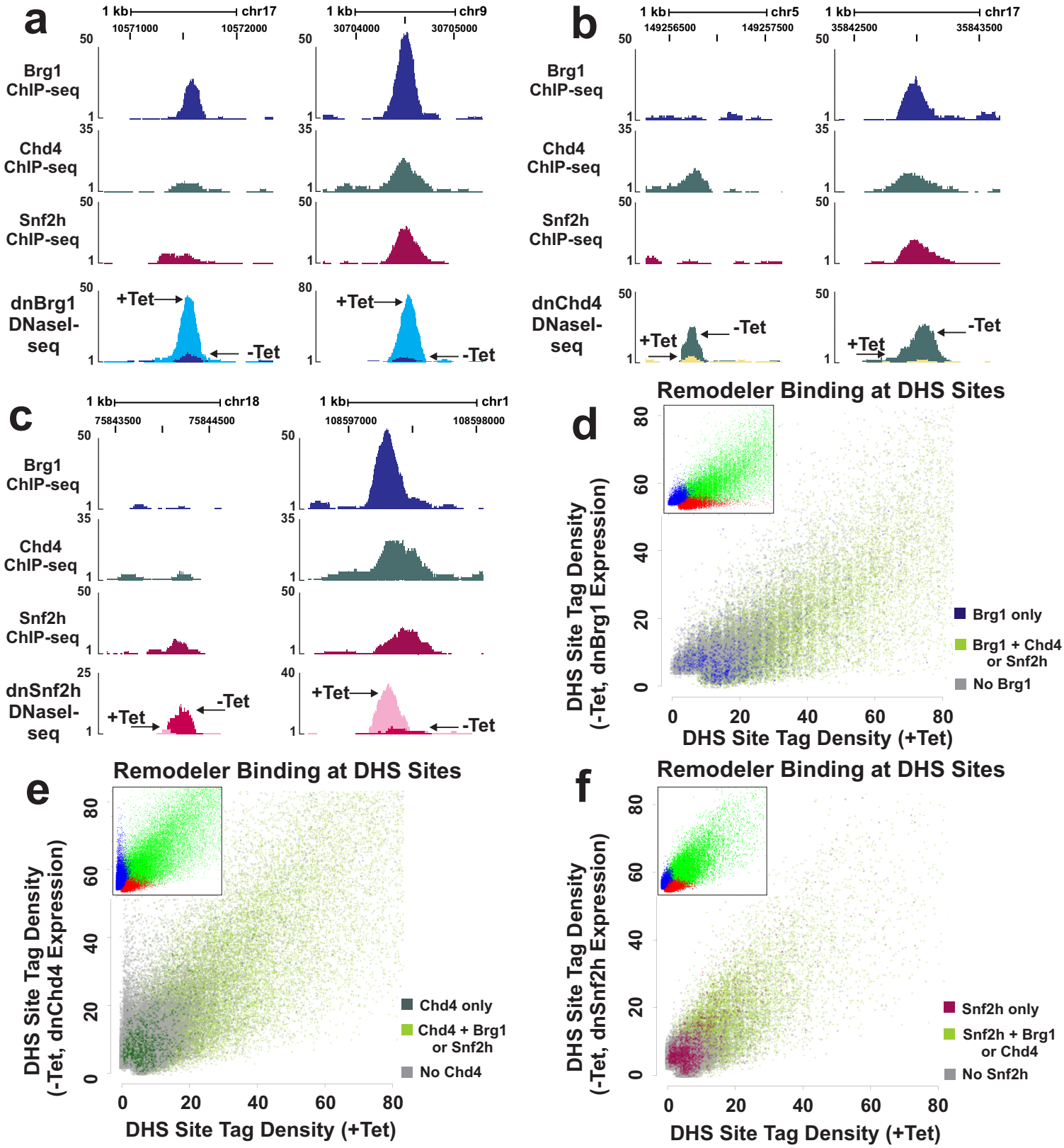

Supplementary Figure 7. Remodeler Binding at Affected DHS Sites (a-c) Genome browser views of ChIP-seq remodeler binding at DNase I hypersensitive (DHS, DNaseI-seq) sites affected by dominant-negative remodeler expression. In each image tag densities are displayed relative to the indicated genomic coordinates. The left image is an example of an affected site bound only by the wild-type version of the mutant remodeler. The right image displays binding by all three remodelers at the affected DHS site. Changes in hypersensitivity in the absence (+Tet) or presence (-Tet) of the indicated dominant-negative remodeler are overlayed and highlighted by arrows. (d-f) Overlay of remodeler binding at DHS sites in the presence or absence of the indicated dominant-negative remodeler protein. Displayed are scatter plots of DHS site tag density in the presence of each dominant-negative protein (y-axis) compared to DHS site tag density in the absence of this protein. Inset, original scatter plots of DNase I hypersensitivity from Fig. 5.

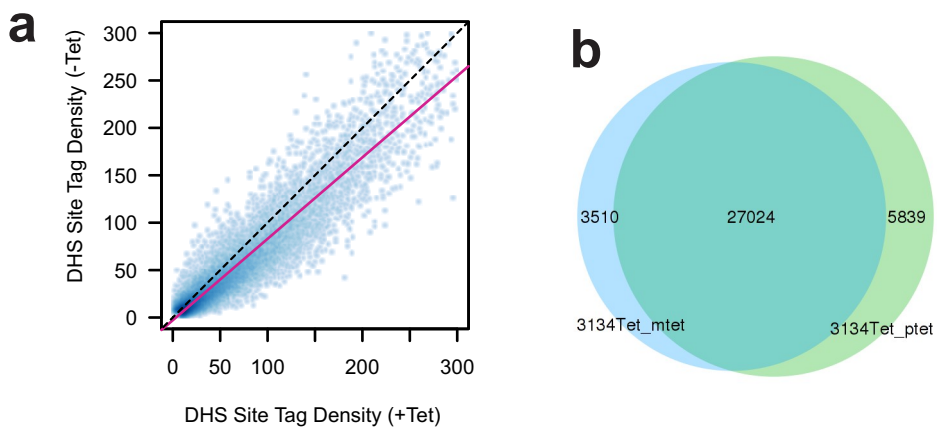

Supplementary Figure 8. Control DHS Data Analysis for Remodeler Binding at Affected DHS Sites

(a) The scatter plot compares the maximum tag density of -Tet versus +Tet DHS hotspots in the control 3134 dataset. (b) The venn diagram shows the overlap between -Tet DHS hotspots and +Tet DHS hotspots in the control 3134 dataset. The area of each subset is proportional to the number of sites.

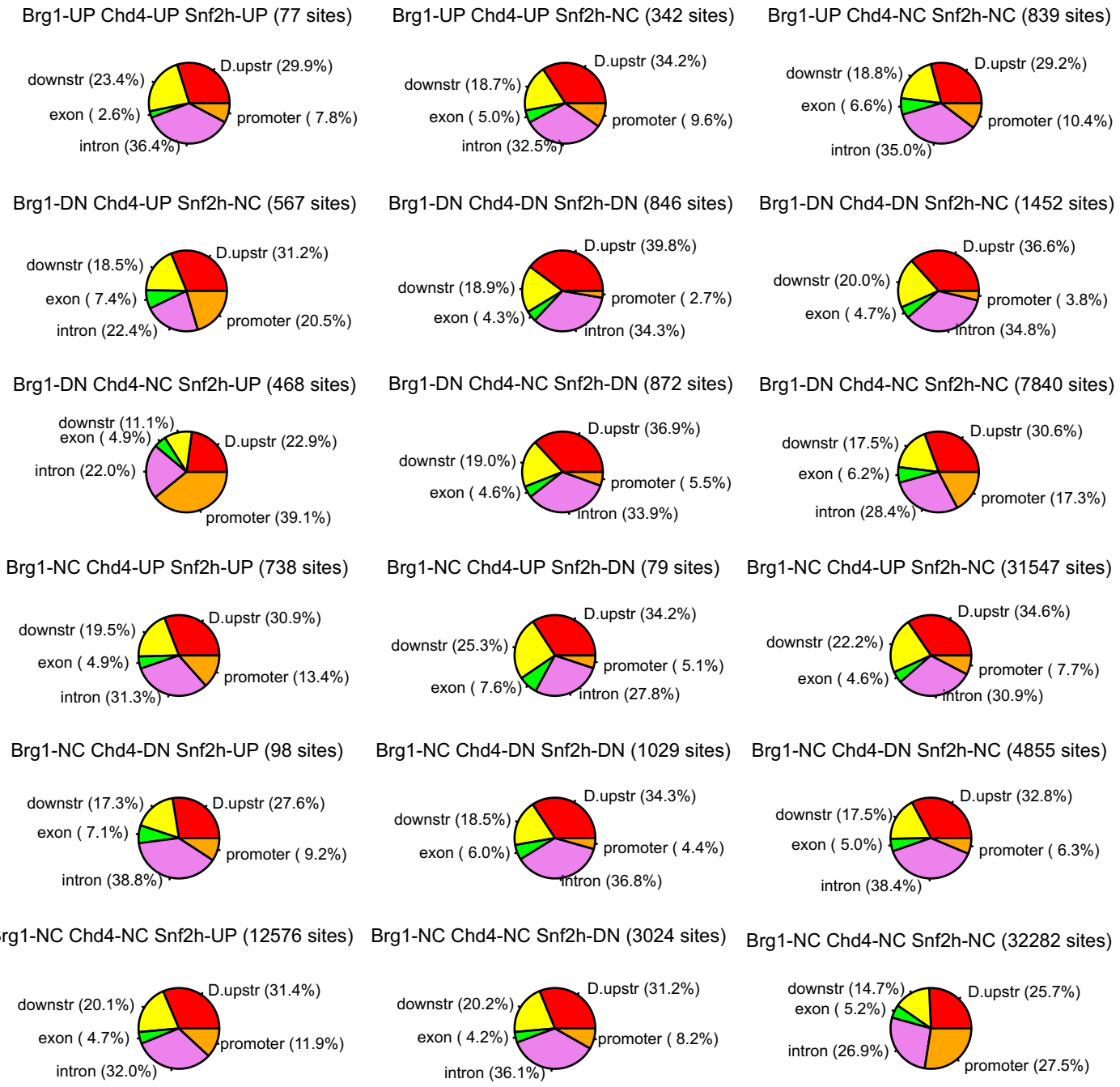

Supplementary Figure 9. Positional distribution for trend classes in chromatin access at DHS sites.
Venn diagrams present the occurrence frequencies for the 27 trend classes expected for dnBrg1, dnSnf2h and dnChd4 interactions at DHS sites. For each of these classes, the positional distribution is shown here for categories with more than 50 sites genome-wide. Notation; Brg1-UP indicates sites increased by more than 2-fold in -Tet (with dnBrg1 expression); Brg1-DN indicates means sites decreased by more than 2-fold in -Tet; NC indicates no change. The same notation is used for the dnSnf2h and dnChd4 classes. Sites are classified as promoter (< 2.5 kb upstream or downstream from the nearest TSS), exon (> 2.5 kb downstream from the nearest TSS , overlapping an exon), intron (> 2.5 kb downstream from the nearest TSS , in an intron not overlapping an exon), distal upstream (> 2.5 kb upstream from the nearest TSS), or downstream (> 2.5 kb downstream from the nearest TSS).

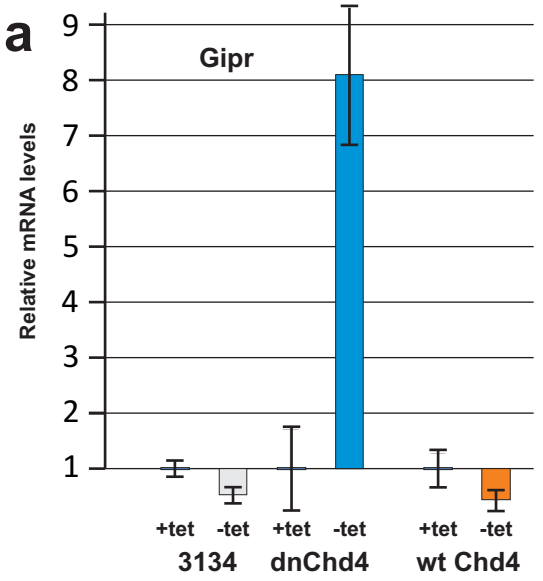

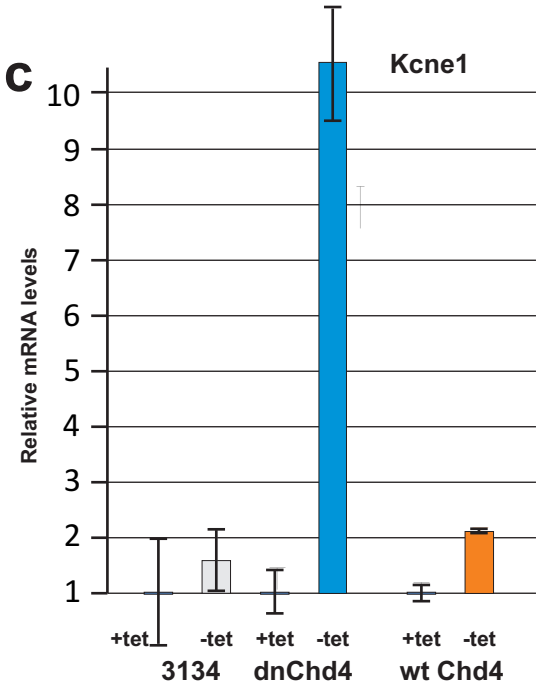

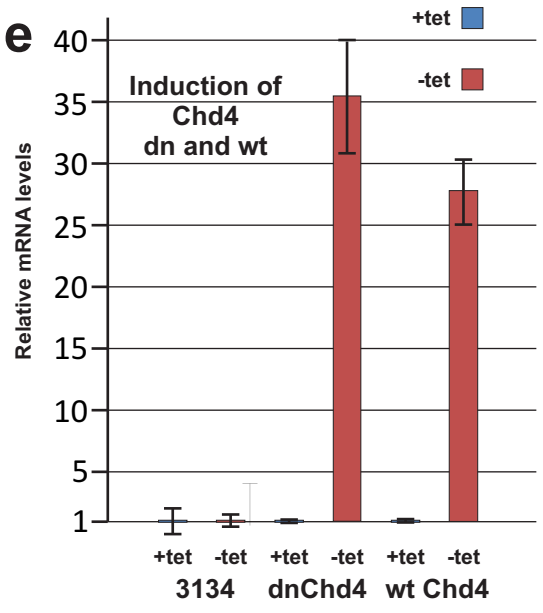

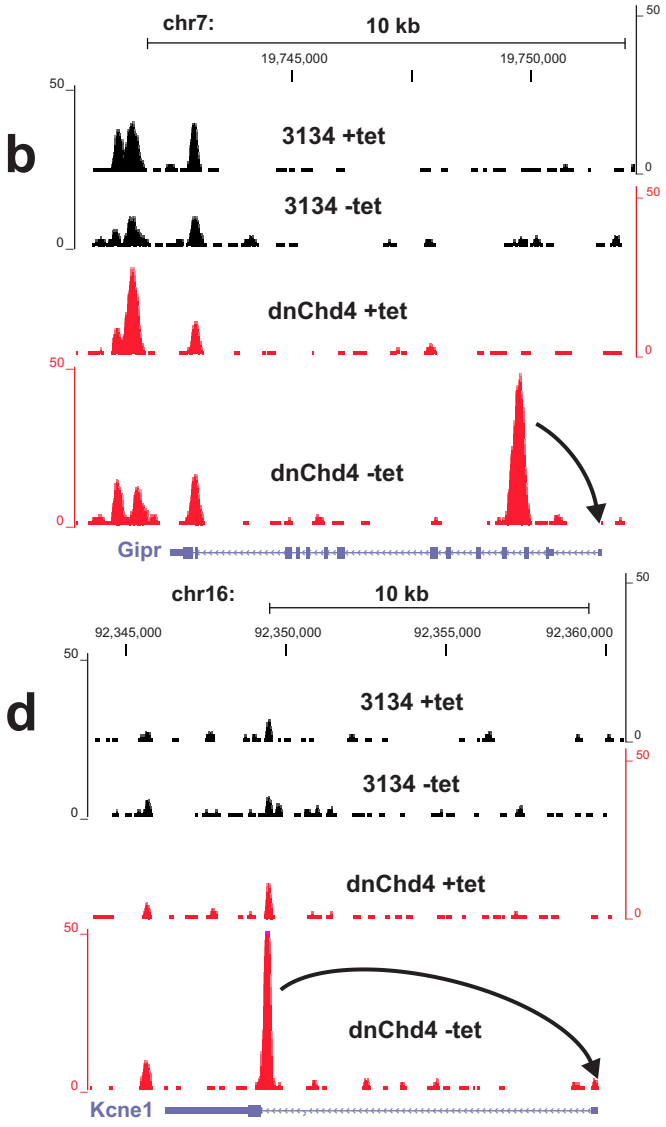

f

	dnBrg1	dnChd4	dnSnf2h	
	329	316	168	Differentially regulated
	145	113	48	Up regulated
	184	203	120	Down regulated

Supplementary Figure 10. Effects of dn-Remodeler Expression on Gene Expression. RNA levels were examined by microarray analysis in cells either expressing (- tet), or not expressing (+tet) dnBrg1, dnSnf2h, and dnChd4. (a) Example 1; Gipr locus is strongly up-regulated by dnCHD4. In a parallel cell line with tet regulated w.t. Chd4, strong induction of the w.t. protein has no effect of Gipr exression. (b) DHS track for Gipr locus; pronounced DHS element immediately downstream of TSS (arrow) is activated by dnCHD4. (c) Example 2; Kcne1 locus is up-regulated by dnCHD4. Again, w.t. Chd4 has no effect. (d) DHS track for Kcne1 locus; DHS element downstream of TSS (arrow) is activated by dnCHD4. (e) In parallel cell lines, -tet activation produces 30-35 fold increases in dnChd4 and w.t. Chd4 RNA levels. (f) Global effects on gene expression. The number of genes either up- or down-regulated (fc > 1.2; $p<0.05$) is shown.

Supplementary Table 1.

Occurrence frequencies for trends in chromatin access at DHS sites
dnBrg1, dnSnf2h and dnChd4 interaction classes

Fold Change = 2.0

Chd4 Increased		(%)	Chd4 Decreased		(%)	Chd4 No Change		(%)
Brg1 Increased								
Snf2h Inc.	77	0.08%	Snf2h Inc.	1	0.00%	Snf2h Inc.	39	0.04%
Snf2h Dec.	2	0.00%	Snf2h Dec.	2	0.00%	Snf2h Dec.	13	0.01%
Snf2h No. Chg	342	0.34%	Snf2h No. Chg	16	0.02%	Snf2h No. Chg	839	0.84%
Brg1 Decreased								
Snf2h Inc.	41	0.04%	Snf2h Inc.	24	0.02%	Snf2h Inc.	468	0.47%
Snf2h Dec.	8	0.01%	Snf2h Dec.	846	0.85%	Snf2h Dec.	872	0.87%
Snf2h No. Chg	567	0.57%	Snf2h No. Chg	1452	1.46%	Snf2h No. Chg	7840	7.87%
Brg1 No Change								
Snf2h Inc.	738	0.74%	Snf2h Inc.	98	0.10%	Snf2h Inc.	12576	12.62%
Snf2h Dec.	79	0.08%	Snf2h Dec.	1029	1.03%	Snf2h Dec.	3024	3.03%
Snf2h No. Chg	31547	31.65%	Snf2h No. Chg	4855	4.87%	Snf2h No. Chg	32282	32.39%

All identified DHS sites from the three dominant negative cell lines (either induced -tet or repressed + tet) were pooled for a total of 99,677 DHS sites. In each cell line, the effect of activation of the given dn-remodeler on each site was scored. There are 27 trend classes expected for all possible dnBrg1, dnSnf2h and dnChd4 interactions at DHS sites (examples presented in Fig. 7, a-k). The number of sites found for each class was calculated with a minimum 2-fold increase, or minimum 2-fold decrease, in tag density upon expression of the dn-remodeler. Sites with a lesser extent of change were classified as no change, NC.

Supplementary Table 2.

Experimental replicates for ChIP seq and DHS seq

Type of Exp	Cell line	Antibody	Biological Replicates	Sequencing Replicates	No. Reads
ChIP	3134	Brg1	Rep 1.	2	17,275,216
ChIP	3134	Brg1	Rep 2.	3	63,275,619
ChIP	3134	CHD4	Rep 1.	2	28,877,292
ChIP	3134	CHD4	Rep 2.	2	40,487,213
ChIP	3134	Snf2h	Rep 1.	3	42,326,935
ChIP	3134	Snf2h	Rep 2.	1	14,447,158
input	3134	NA		1	5,954,325
input	3134	NA		1	21,065,317
DHS	3134+tet			2	32,836,139
DHS	3134-tet			2	39,361,691
DHS	3134+tet (DNBrg1)			2	17,455,054
DHS	3134-tet (DNBrg1)			2	40,227,690
DHS	3134+tet(DNCHD4)			3	57,669,433
DHS	3134-tet(DNCHD4)			3	51,963,930
DHS	3134+tet(DNSnf2h)			2	54,764,150
DHS	3134-tet(DNSnf2h)			2	50,090,775

Biological and technical replicate sequencing datasets are listed for the results presented in this manuscript.